Mon. Not. R. Astron. Soc. **000**, 1–5 (2006) Printed 1 February 2007 (MN LATEX style file v2.2)

Bubbles as tracers of heat input to cooling flows

J. Binney, F. Alouani Bibi⋆, H. Omma
St Johns Research Centre, 45 St Giles, Oxford, OX1 3JP, UK

Submitted 2006, November 21

ABSTRACT
We examine the distribution of injected energy in three-dimensional, adaptive-grid simulations of the heating of cooling flows. We show that less than 10 percent of the injected energy goes into bubbles. Consequently, the energy input from the nucleus is underestimated by a factor of order 6 when it is taken to be given by $PV\gamma/(\gamma-1)$, where P and V are the pressure and volume of the bubble, and γ the ratio of principal specific heats.

Key words: cooling flows – galaxies: clusters: general – galaxies: formation

1 INTRODUCTION

It is now widely accepted that bipolar outflows from active galactic nuclei (AGN) largely offset the radiative losses of the hot plasma that forms "cooling flows" – systems in which there is a central depression in the temperature of the gravitationaly trapped plasma (Binney 2005; Donahue et al. 2006). Notwithstanding this concensus about the importance of AGN for cooling-flow evolution, considerable controversy surrounds the mechanisms by which AGN heat cooling flows.

Observations, first by ROSAT (Böhringer et al. 1993) and later by Chandra (Fabian et al. 2001) of regions of depressed X-ray emission and (usually) enhanced synchrotron emission, have played a crucial role in overturning the paradigm of distributed mass dropout that dominated the field in the 1980s and 1990s. These regions have been called "bubbles" and considerable effort, both numerically (Churazov et al. 2000; Brüggen et al. 2002) and theoretically (Churazov et al. 2002; Roychowdhury et al. 2004, 2005) has been devoted to understanding the way bubbles interact with the surrounding, higher-density plasma.

Since lines of sight through a bubble also pass through large volumes of X-ray emitting plasma in front of and behind a bubble, even a weak depression in the X-ray surface brightness at the location of the bubble may be indicative of a large drop in emissivity inside the bubble. In fact Fabian et al. (2000) report that the data for the Perseus cluster are consistent with zero emissivity inside one of the bubbles. Consequently, it is generally assumed that inside bubbles the density of thermal plasma is so low that the plasma emits negligibly in X-rays. This material is generally assumed to be matter shot out from the nucleus in a high-velocity jet, which was thermalized to a high temperature in the hotspot that marks the interface between the jet and shocked ambient plasma.

Given that the plasma is close to an ideal gas, the thermal energy inside a bubble is $U = PV/(\gamma-1)$, where γ is the ratio of principal specific heats. By taking the bubble to be in pressure balance with the X-ray emitting plasma immediately outside it, P can be determined from the X-ray data, while V follows from the geometry. Hence the energy *inside* bubbles can be reliably estimated from observational data.

During inflation of a bubble work is inevitably done on the surroundings plasma. The *minimum* work that must be done at this stage is the work that would be done if the bubble expanded reversibly, which is PV, bringing the minimum energy associated with a bubble to $\gamma/(\gamma-1)PV = \frac{5}{2}PV$ for a non-relativistic plasma ($\gamma = \frac{5}{3}$). However, the inflation of bubbles is probably anything but reversible, and in this case, by Clausius' inequality the work done will exceed PV. We use high-quality hydrodynamical simulations of bubble formation to examine how much work is actually done by the jet, and conclude that it exceeds $\frac{5}{2}PV$ by a substantial factor.

2 THE SIMULATIONS

The framework within which we simulate cluster heating has been described elsewhere (Omma et al. 2004; Omma & Binney 2004). We use the adaptive-grid Eulerian hydrocode ENZO (Bryan & Norman 1997) with a piecewise-parabolic Riemann solver. The plasma is assumed to be an ideal, monatomic, non-relativistic gas. Radiative losses are calculated in the optically-thin limit using the line and continuum cooling rates of Sutherland & Dopita (1993).

The initial conditions are modelled on the current con-

⋆ E-mail: binney@thphys.ox.ac.uk; alouani@astro.ox.ac.uk

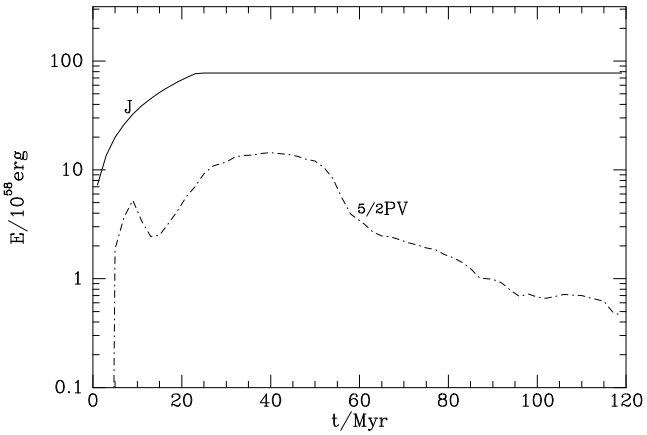

Figure 1. The full curve shows the energy actually injected by the jets, while the broken curve shows the energy associated with bubbles.

figuration of the Hydra cluster as determined from Chandra data by David et al. (2001). Jets are launched by depositing mass, momentum and energy in an injection disk of radius 3 kpc (Omma et al. 2004). The grid cells are cubical and 0.6 kpc on a side at the centre, growing in stages by a factor of two in side length up to 36 kpc at the edge of the grid, which is a cube 614 kpc on a side. Periodic boundary conditions are imposed on this outer boundary. In contrast to many other simulations of cluster heating (e.g., Basson & Alexander 2003; Heinz et al. 2002; Vernaleo & Reynolds 2006) there is no inner boundary.

We have analyzed the energetics of all the simulations described in Omma & Binney (2004). These differed in the amount of time the cluster cooled passively before jet igniton, and in the power and duration of the jets, as well as in whether there was more than one episode of jet ignition. However, we found similar energetics of bubbles in all simulations, so here we present only results from simulation S2, in which the cluster cooled passively for 300 Myr before a pair of jets with combined power $10^{45}\,\mathrm{erg\,s^{-1}}$ ignited and ran for 25 Myr.

3 RESULTS

In a series of snapshots bubbles were identified as regions in which the density was a factor f smaller than the mean density at that radius, and the volume V of the bubbles determined as a function of f. Clearly V is zero for $f = 0$ and is comparable to the total available volume for $f = 1$. For $0.2 \lesssim f \lesssim 0.75$ there is a plateau in V that we identify with the bubbles, and we present results obtained by adopting $f = 0.3$.

In Fig. 1 the full curve shows as a function of time since jet ignition the energy injected into the simulation, while the dashed curve shows $\frac{5}{2}PV$ for the bubbles. The energy associated with the bubbles peaks at 14×10^{58} erg, while the energy injected is 78×10^{58} erg. Thus less than a fifth of the injected energy is ever associated with identifiable bubbles, and at most epochs the fraction is less.

To answer the question "where *is* the energy?" we have analysed the volume within 200 kpc of the cluster centre in the following way. We grouped the computational cells into approximately 40 spherical shells and in each shell i calculated

$$\Delta E_i = \sum_{\text{cells } \alpha} V_\alpha [e_\alpha(t) - e_\alpha(0)], \qquad (1)$$

where V_α is the volume of the αth cell and e_α is an energy density within that cell. The energy densities considered were $u = \frac{3}{2} n k_{\rm B} T$, where n is the particle density, $w = -\rho\Phi$, where ρ is the matter density and $\Phi < 0$ is the gravitational potential, and $k = \frac{1}{2}\rho v^2$, where v is the flow speed. In this way we obtain measures ΔU, ΔW and ΔK of the changes since jet ignition in internal, potential and kinetic energy within each shell.

t/Myr	ΔU	ΔK	ΔW	ΔE	ΔU	ΔK	ΔW	ΔE
25	-11	2	-132	123	64	8	160	-88
50	-54	9	-143	98	90	4	215	-120
75	-62	15	-82	34	95	3	223	-125
85	-63	16	-60	13	98	2	211	-111

Table 1. Energy changes (in units of 10^{58} erg) in the radius ranges $(0, r_{\rm cavity})$ (columns 2 to 5) and $(r_{\rm cavity}, r_{\rm shock})$ (columns 6 to 9). The values of $r_{\rm cavity}$ are 15, 37, 58 and 70 kpc, while those of $r_{\rm shock}$ are 35, 75, 100 and 115 kpc. $\Delta E \equiv \Delta U + \Delta K - \Delta W$.

Fig. 2 gives the radial distribution of energy differences at four times, 25, 50, 75 and 85 Myr after jet ignition. At 25 Myr (top left panel) the jets have just switched off and the curves are structured by two distinct processes. At $r \lesssim 30$ kpc the jets are dominant, producing sharp peaks in internal (full curve), potential (short-dashed curve), and kinetic energy (dotted). Interior to the peak in potential energy ΔW at $r \simeq 20$ kpc, there is a region in which $\Delta W < 0$ because uplift has reduced the mass density there. In this region the internal energy is only very slightly depressed because the drop in ρ is compensated by a rise in T. Beyond ~ 40 kpc the curves for ΔU and ΔW are structured by radiative cooling, which causes a slow decline in T and a flow of material from large to small radius that causes ΔW to be positive at $r \lesssim 150$ kpc and negative further out.

The long-dashed curve in the top left panel shows the radiated energy R: unlike the other curves, this is not calculated by differencing energy densities at two epochs but by integrating the X-ray emissivity j_X through the volume of each cell and with respect to time since jet ignition.

The top right panel of Fig. 2 shows the disposition of energy 50 Myr after jet ignition. Compared to the top left panel for $t = 25$ Myr, the long-dashed curve of the radiative losses has risen at all radii, and the peaks in ΔU, ΔW and ΔK have moved outwards with the rising jet debris. Now the curves for ΔU, ΔW and ΔK are structured by the jet for $r \lesssim 70$ kpc and by cooling further out. At small radii the peak in ΔU is now preceeded by a pronounced trough, reflecting the development of an under-pressured region behind the zone filled by material that is being carried up by its momentum, and decelerating in the cluster's gravitational field. At $r \gtrsim 80$ kpc cooling continues to drive an inward flow that makes the negativity of ΔU and ΔW at large radii more pronounced.

The bottom left panel of Fig. 2, for $t = 75$ Myr after jet ignition, shows a new feature: the curves for ΔU and especially ΔW have developed peaks at $r \simeq 20$ kpc, interior

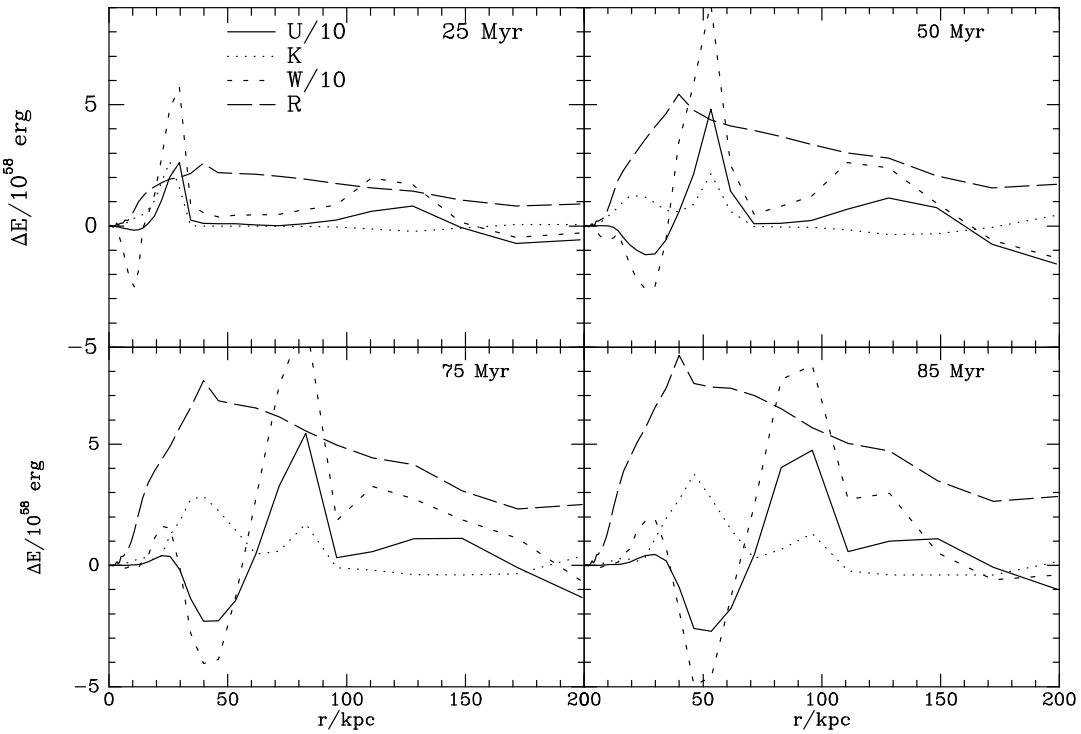

Figure 2. The radial distribution of energy changes defined by equation (1) since jet ignition.

to the troughs that preceed the main peaks. This new region of enhanced potential energy reflects material that has fallen down after being uplifted and is now at a radius lower than the radius it would have in an equilibrium model, given its specific entropy. Thus this peak reflects a particular phase of the gravity waves that are strongly excited by the jets. The bottom-right panel, for $r = 85$ Myr is very similar to that for 75 Myr.

At each panel of Fig. 2 one can identify two characteristic radii, namely the radius $r_{\rm shock}$ that marks the end of the sharp drop in curves for ΔU and ΔW that the shock produces, and the radius $r_{\rm cavity}$ at which these curves cross zero on the other side of the peak. For the time of each panel in Fig. 2, Table 1 gives energies, in units of 10^{58} erg, contained in the regions $r < r_{\rm cavity}$ and $r_{\rm cavity} < r < r_{\rm shock}$. We see that at 25 Myr, as the jet shuts off, the total energy inside $r_{\rm cavity}$ has increased by an amount $\Delta E = \Delta U + \Delta K - \Delta W = 123 \times 10^{58}$ erg, that greatly exceeds the total injected energy, $E_{\rm jet} = 78 \times 10^{58}$ erg and is more than an order of magnitude greater than the energy then associated with bubbles (8.9×10^{58} erg from Fig. 1). This energy increase is largely caused by a negative value of $\Delta W = -132 \times 10^{58}$ erg following uplift of material – to achieve this value, the jet has not in fact supplied 132×10^{58} erg of energy, which would suffice to lift the uplifted material to $r = \infty$, but only the smaller amount required to move material out of the cavity zone. This explains why ΔE for this region exceeds the the jet energy. In the dense region outside $r_{\rm cavity}$ and inside $r_{\rm shock}$, ΔW has increased by twice the jet energy, reflecting (i) the arrival from below of gravitationally bound uplifted material, and (ii) the arrival from above of material that has cooled. The internal energy of the gas in this region has risen by 75% of $E_{\rm jet}$. At this stage the bulk kinetic energy alone is equal to the energy associated with bubbles.

At later times we see that within $r_{\rm cavity}$, ΔU and ΔK continue to increase, while ΔW becomes less negative. In the dense shell further out ΔK continually decreases, while ΔU slowly rises. The total energy change ΔE in the dense shell is always falling as material is driven in by the jet-induced flow on one side and gravity on the other, bringing with it large (negative) potential energies. In this region cooling also attenuates the rise in ΔU that would otherwise occur.

4 DISCUSSION

We have shown that in the simulations the minimum energy associated with bubbles, $E_{\rm min} = \frac{5}{2}PV$, is smaller than the injected energy by at least a factor of nearly 6. Why is this so, and can we expect the result to extend to real cooling flows, or does it merely reflect limitations of the simulations?

The factor $\frac{5}{2}$ allows for the energy $\frac{3}{2}PV$ that is actually in the bubble, and an allowance PV for the work that must be done to create a cavity in the ambient medium. As explained in the Introduction, this is the *minimum* allowance, and is the actual requirement only if the cavity is created reversibly and at constant pressure. In this case the displaced material would be neither heated nor accelerated, and the work PV would be done on the mechanism (piston etc) that held the pressure constant. In reality the creation of the cavity is strongly irreversible, so the displaced material is heated and accelerated. In as much as real jets probably involve larger velocities than those ($\sim 40\,000\,{\rm km\,s^{-1}}$) characteristic of the simulations, the simulations may be expected to under- rather than over-estimate the irreversibility of bubble inflation.

The internal energy of displaced material is changed by of order itself, and its original value was equal to the bubble energy. Moreover the material evacuated from the cavity itself displaces material, so the mass of the material that has to be moved and heated exceeds the mass originally associated with the cavity by a factor $\alpha > 1$, say. Doubling the internal energy of the shifted material, would involve supplying $\frac{3}{2}\alpha PV$ of energy over and above what is required in the reversible case.

In the simulations the timescale for bubble inflation is of order the sound-crossing time at the ambient sound speed, and it is widely assumed that the same is true in real clusters. Consequently, the shifted material inevitably gains an amount of kinetic energy that is comparable to the original internal energy, $\frac{3}{2}\alpha PV$, as Table 1 confirms to be the case.

These two estimates of energy that must be supplied should be added to the energy $\gamma PV/(\gamma-1)$ required in the reversible case, where γ is the ratio of principal specific heats of the material in the cavity. In our simulations $\gamma = \frac{5}{3}$, so the actual energy required is larger than the minimum energy by a factor $1+\frac{6}{5}\alpha$. If the cavity contains relativistic plasma, as is frequently assumed, and the ambient plasma is non-relativistic, the energy that must be supplied is larger than the minimum energy by a factor $1+\frac{3}{4}\alpha$. The energetics of the simulations implies that the shifted mass is $\alpha = 3.75$ times the mass originally in the bubble

In reality α is probably not so large because diffusivity will lead to PV being underestimated, both in the simulations and in real cooling flows. Our simulations do not explicitly include thermal conductivity, but any numerical hydrodynamic scheme has significant diffusivity on the scale of the grid (or the mean-free path in the case of smooth-particle hydrodynamics) by virtue of assigning single values to the dynamical variables at each grid point, when in reality the material in a cell would contain hot and cold regions. As a consequence, energy can cross a cell in one timestep when hot matter enters on one side at the start of a timestep, and warmed matter leaves on the opposite side at the start of the next timestep. There is no concensus regarding the appropriate values of the kinetic transport coefficients of intracluster gas [see Kim & Narayan (2003); Pope et al. (2005) for conflicting positions], and even less understanding of the effectiveness of turbulent transport. However, turbulence stretches and distorts bubbles, and when their narrowest dimension becomes comparable to the grid spacing, diffusivity will eliminate them. Thus kinetic and turbulent diffusivity cause bubbles to shrink on a dynamical timescale in the simulations, as they probably do in reality

The broken curve in Fig. 1 illustrates this phenomenon at two points: between $t \simeq 8$ and 14 Myr, PV dips while the jet is still firing, and then at $t > 50$ Myr it falls continuously after the jet has switched off. The dip at early times reflects shrinkage in the volume of low-density material by ~ 25 percent following the emergence of turbulent eddies around the jet; as the jet establishes itself at $t \approx 7$ Myr, the cavities shift from being nearly hemispherical to elongated (Fig. 3). The steep velocity gradient perpendicular to the jet axis then induces large-scale turbulence, which draws cool material into the cavity. The ensuing fragmentation of the cavity leads to the decline in cavity volume that causes the dip in the PV curve of Fig. 1. At $t > 14$ Myr a new regime is entered in which lobes swell around the now more slowly advancing

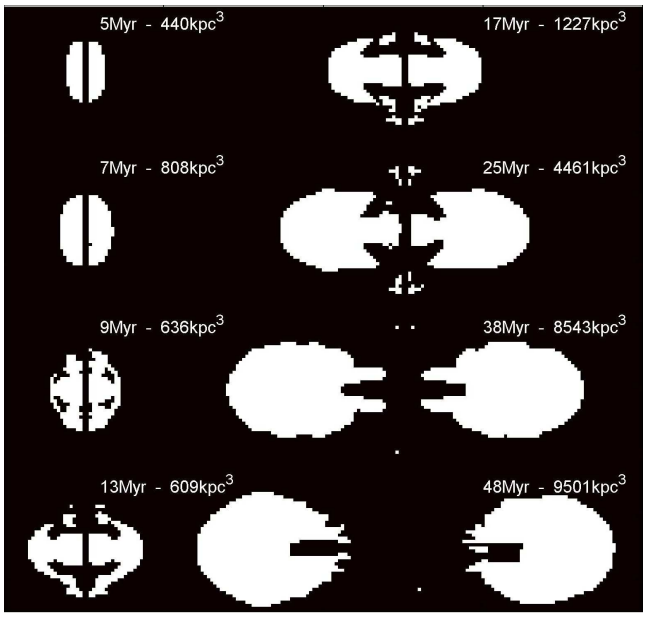

Figure 3. Cross sections through the cavities at eight times. In addition to the time since jet ignition, each panel gives the total volume of the cavities. Note that there are scale changes between images.

hotspots. The drop in the PV curve at $t > 50$ Myr is also driven by turbulent breakup. How realistic the steepness of this drop is, we do not know.

Observationally it is inevitable that the volume of cavities will be underestimated because it has been determined from X-ray surface brightness, rather than from a knowledge of the plasma density at each point in three dimensions, as can be done in the simulations. Clearly such underestimation of the volume will lead to a corresponding underestimation of the power input by the jets. It would be interesting to compare estimates of cavity volumes obtained from X-rays with ones obtained from high-resolution radio maps, which might be less sensitive to projection effects. On the other hand, the X-ray cavities sometimes do not coincide with the radio lobes – the Hydra cluster provides an example of this phenomenon (Nulsen et al. 2005).

This discussion leads to the conclusion that taking the energy injected by jets to be $\frac{5}{2}PV$ probably does lead to its being underestimated by a substantial factor, which we have estimated to be ~ 5.5. Our estimate of this factor may be on the high side if the simulations over-estimate the diffusivity of the plasma that arises from both turbulent mixing and kinetic processes, but may be on the low side because our jet speeds are relatively low and cavity volumes are likely to be underestimated from X-ray surface brightnesses.

The fact that most of the injected energy is never in cavities, has important implications for the time- and space-dependence of cluster heating. As Table 1 shows, much of this energy is stored as potential energy – the energy required to lift low-entropy gas above its natural position in the cluster atmosphere. This energy subsequently heats the plasma through the dissipation of the non-linear gravity waves to which it gives rise. The timescale of this release can be very long, especially in the case of an unusually violent outburst of the AGN, which drives cool plasma

to great heights, at which the dynamical time can be long (Omma et al. 2004).

Several studies (e.g., Birzan et al. 2204; Nipoti & Binney 2005; Best et al. 2006; Allen et al. 2006) have considered the implications of cooling flows for the phenomenolgy of AGN and radio sources under the assumption that the injected energy is $\gamma PV/(\gamma - 1)$. The studies conclude that heating by AGN can balance radiative cooling provided the duty cycle of the jets is high. With our increased estimate of the energy injected in a given episode of bubble inflation, the required duty cycles will be shorter.

Assuming a 10 percent efficiency in the conversion of rest mass to jet power, Allen et al. (2006) conclude that jet powers are smaller than the rate of energy release from Bondi accretion of hot plasma by a factor ~ 6 (their Fig. 4). Prima facie, our increase in the required jet power would bring it up to the rate of release of energy by Bondi accretion. Is this conclusion problematic, given that only a fraction of the plasma that passes over the Bondi accretion radius can be swallowed by the black hole?

The rate at which material passes the Bondi radius provides a useful measure of the mean jet power, but not of the instantaneous power, because inside the Bondi radius an accretion disc is likely to provide a reservoir of material, and jet outbursts are thought to be brief episodes in the evolution of this disc (Nipoti et al. 2005; Koerding et al. 2006). Thus on the timescale of bubble inflation, jet power can safely exceed the mean power available by Bondi accretion, even if the black hole's only mass supply is from virial-temperature gas (which is by no means certain). Estimates of the power available from Bondi accretion are most usefully compared with the radiative losses of the cooling flow (Binney 2005).

ACKNOWLEDGMENTS

This work has been supported by St Johns College, Oxford

REFERENCES

Allen, S.W., Dunn, R.J.H., Fabian, A.C., Taylor, G.B., Reynolds, C.S., 2006, MNRAS, 372, 21
Basson J.F., Alexander P., 2003, MNRAS, 339, 353
Best P.N., Kaiser C.R., Heckman T.M., Kauffmann G., 2006, MNRAS, 368, 67
Binney, J., 2005, Phil. Trans. roy. Soc., 363, 739 (astro-ph/0407238)
Birzan L., Rafferty D.A., McNamara B.R., Wise M.W., Nulsen P.E.J., 2004. ApJ, 607, 800
Böhringer H., Voges W., Fabian A.C., Edge A.C., Neumann D.M., 1993, MNRAS, 264, L25
Brüggen M., Kaiser C.R., Churazov E., Ensslin T.A., 2002, MNRAS 331, 545
Bryan G.L., Norman M.L., 1997, in "Computational Astrophysics", ASP Conf. Ser. 123, p. 363
Churazov E., Forman W., Jones C., Böhringer H., 2000, A&A, 356, 788
Churazov E., Sunyaev, R., Forman, W., Böhringer H., 2002, MNRAS, 332, 729
Churazov E., Forman W., Jones C., Böhringer H., 2003, ApJ, 590, 225
Donahue, M., Horner, D.J., Cavagnolo, K.W., Voit, G.M., 2006, ApJ, 643, 730
David L.P., Nulsen P.E.J., McNamara B.R., Forman W., Jones C., Ponman T. Robertson B., Wise M., 2001, ApJ, 557, 546
Fabian, A.C., Sanders, J.S., Ettori, S., Taylor, G.B., Allen, S.W., Crawford, C.S., Iwasawa, K., Johnstone, R.M., Ogle, P.M., 2000, MNRAS, 318, 65
Fabian A.C., Mushotzky R.F., Nulsen P.E.J., Peterson J.R., 2001, MNRAS, 321, L20
Heinz, S., Choi, Y.-Y., Reynolds, C. S. & Begelman, M. C. 2002, ApJ, 569, L79
Kim, W.-T., Narayan R., 2003, ApJ, 596, 889
Koerding E., Jester S., Fender R., 2006, MNRAS, 372, 1366
Omma, H. & Binney, J. 2004 MNRAS, 350, L13
Omma, H., Binney, J., Bryan, G., Slyz, A., 2004, MNRAS, 348, 1105
Nipoti C., Binney J., 2005, MNRAS, 361, 428
Nipoti C., Blundell K., Binney J., 2005, MNRAS, 361, 633
Nulsen P.E.J., Hambrick D.C., McNamara B.R., Rafferty D., Birzan L., Wise M.W., David L.P., 2005, ApJ, 625, L9.
Pope E.C.D., Paylovski G., Kaiser C.R., Fangohr H., 2005, MNRAS, 364, 13
Roychowdhury, S., Ruszkowski, M., Nath, B.B., Begelman, M.C., 2004, ApJ, 615, 681
Roychowdhury, S., Ruszkowski, M., Nath, B.B., 2005, ApJ, 634, 90
Sutherland, R.S., Dopita, M.A., 1993, ApJS, 88, 253
Vernaleo, J.C., Reynolds, C.S., 2006, ApJ, 645, 83